On the role of membrane anisotropy in the beading transition of undulated tubular membrane structures

Aleš Iglič[1], Blaž Babnik[1], Ulrike Gimsa[2] and Veronika Kralj-Iglič[3,1]

[1] Laboratory of Physics, Faculty of Electrical Engineering, University of Ljubljana, Tržaška 25, SI-1000 Ljubljana, Slovenia
[2] Neurobiological Laboratory, Department of Neurology, University of Rostock, Gehlsheimer Str 20, D-18147 Rostock, Germany
[3] Institute of Biophysics, Faculty of Medicine, University of Ljubljana, Lipičeva 2, SI-1000 Ljubljana, Slovenia

Abstract
The Helfrich expression for the isotropic membrane bending energy was generalized for the case of anisotropic membranes by taking into account two intrinsic (spontaneous) curvatures, i.e., the intrinsic mean curvature H_m and the intrinsic curvature deviator D_m. Using this generalized expression for the membrane bending energy the shape equation for closed axisymmetric anisotropic membranes is solved numerically for the case of undulated tubular shapes. It is shown that the variation of one of the two intrinsic curvatures, H_m or D_m, may induce the first-order-like shape transitions between the undulated tubular membrane structures. The predicted discontinuous shape transitions were applied to explain the beading transitions without stretching, which were recently observed in nerve fibres.

PACS numbers: 05.07.Np, 87.16.Dg

1. Introduction

Thin shells and strips are in general anisotropic [1–3] and can attain various equilibrium shapes which are not flat or spherical. For isotropic thin films, strips and membranes the equilibrium shapes were usually determined by the minimization of isotropic bending energy [4]

$$w_b = \frac{k_c}{2}(2H - C_0)^2 + k_G K,\tag{1}$$

where $H = (C_1 + C_2)/2$ is the mean curvature, C_0 is the spontaneous curvature, $K = C_1 C_2$ is the Gaussian curvature, while k_c and k_G are the splay modulus and the saddle-splay
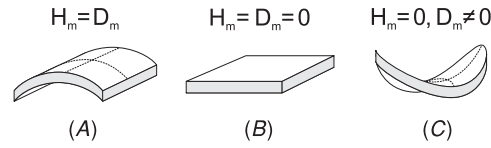
Figure 1. A schematic figure of the most favourable shapes of the small part of the thin membrane (shell) having different values of the intrinsic (spontaneous) mean curvature H_m and intrinsic (spontaneous) curvature deviator D_m.

modulus, respectively. The values of local curvatures corresponding to the extreme of the function w_b (determined from $\partial w_b / \partial C_i = 0$, $i = 1, 2$) are

$$C_1^{eq} = C_2^{eq} = k_c C_0 / (2k_c + k_G). \tag{2}$$

In local thermodynamic equilibrium the above values of curvatures correspond to the local minimum of w_b if $\left[\left(\partial^2 w_b / \partial C_1^2 \right) \left(\partial^2 w_b / \partial C_2^2 \right) - \left(\partial^2 w_b / \partial C_1 \partial C_2 \right)^2 \right] > 0$ (for $k_c > 0$), leading to the well-known local stability condition for a small and completely free (unbound) patch of the membrane $k_c > -k_G/2$ [5].

Equation (1) was used in the modelling of stable anorganic [6] and organic [6, 7] multilayered closed structures. The above expression for the isotropic bending energy was generalized for the case of anisotropic membranes based on the tilt and chirality of membrane components [1, 8, 9] or in-plane orientational ordering of bilayer constituents [2, 10–12]. In this work, we generalize the expression for the bending energy for anisotropic membranes and strips by taking into account the deviatoric elasticity [3]. In the model we introduce two intrinsic (spontaneous) curvatures, i.e., the intrinsic mean curvature H_m and the intrinsic curvature deviator D_m. We show that the variation of the two intrinsic curvatures, H_m and D_m, may explain the beading transition in nerve fibres [13, 14].

2. Free energy

In this work, the membrane (shell) is treated as a two-dimensional surface of a continuum where it is taken into account that it is, in general, anisotropic in two dimensions. It is considered that the elastic energy of a chosen very small surface element of the membrane (shell) is, in the absence of the external forces, equal to zero if its principal curvatures C_1 and C_2 are equal to its intrinsic principal curvatures C_{1m} and C_{2m} (figure 1) and if the orientations of principal systems of the actual local membrane curvature tensor $\underline{C}$ and the intrinsic membrane curvature tensor $\underline{C}_m$ coincide. If a given shape had such principal curvatures and mutual orientation of the principal systems of $\underline{C}$ and $\underline{C}_m$ in all its points, the elastic energy of such shape would be zero [15].

We define the elastic energy per unit area of a very small element of the thin plate with area dA as the energy of mismatch between the actual local membrane curvature of this surface element and its intrinsic (spontaneous) curvature. As already mentioned above the tensor $\underline{C}$ describes the actual curvature while the tensor $\underline{C}_m$ describes the intrinsic curvature, i.e., the curvature which would be energetically the most favourable (figure 1). In the respective principal systems the matrices that represent curvature tensors include only the diagonal elements

$$\underline{C} = \begin{bmatrix} C_1 & 0 \\ 0 & C_2 \end{bmatrix}, \qquad \underline{C}_m = \begin{bmatrix} C_{1m} & 0 \\ 0 & C_{2m} \end{bmatrix}. \tag{3}$$

The principal systems of these two tensors are, in general, rotated in the tangent plane of the surface for an angle ω with respect to each other. The mismatch between the actual local

membrane curvature of the plate and the intrinsic membrane curvature in the absence of the external forces is characterized by the tensor $\underline{M} = \underline{R}\ \underline{C}_m\underline{R}^{-1} - \underline{C}$, where

$$\underline{R} = \begin{bmatrix} \cos\omega & -\sin\omega \\ \sin\omega & \cos\omega \end{bmatrix}. \tag{4}$$

is the rotation matrix.

The small patch of the shell should adapt in order to fit into its place in the actual membrane. This is reflected in the energy that is needed for such deformation. The elastic energy per unit area w is a scalar quantity. Therefore each term in the expansion of w must also be a scalar [16], i.e., an invariant with respect to all transformations of the local coordinate system. In this work, the elastic energy density w is approximated by an expansion in powers of all independent invariants of the tensor $\underline{M}$ of the second order in the components of $\underline{M}$. The trace and the determinant of the tensor are taken as the set of invariants [3],

$$w = \frac{K_1}{2}(\mathrm{Tr}\,\underline{M})^2 + K_2\,\mathrm{Det}\,\underline{M}, \tag{5}$$

where K_1 and K_2 are constants. Taking into account the definition of the tensor $\underline{M}$ it follows from equations (3)–(5) that the energy density w can be written as [15]

$$w = (2K_1 + K_2)(H - H_m)^2 - K_2\big(D^2 - 2DD_m\cos 2\omega + D_m^2\big), \tag{6}$$

where $D = (C_1 - C_2)/2$ is the curvature deviator that is the invariant of the curvature tensor $(D^2 = (\mathrm{Tr}(\underline{C})/2)^2 - \mathrm{Det}(\underline{C}) = H^2 - C_1C_2)$, $H_m = (C_{1m} + C_{2m})/2$ is the intrinsic (spontaneous) mean curvature and $D_m = (C_{1m} - C_{2m})/2$ is the intrinsic (spontaneous) curvature deviator. It can be seen from equation (6) that the material properties of an anisotropic thin membrane (shell) can be expressed in a simple way by only two parameters: the intrinsic mean curvature H_m and the intrinsic curvature deviator D_m. Figure 1 shows schematically cylindrical, flat and saddle-like intrinsic (spontaneous) shapes of the thin membrane (shell).

If the membrane (shell) is isotropic (i.e., $D_m = 0$) equation (6) transforms (up to the constant terms independent on H and D) into the Helfrich expression for the area density of the isotropic bending energy (equation (1)), where $k_c = K_1$, $k_G = K_2$ and

$$C_0 = (2K_1 + K_2)H_m/K_1 = (2k_c + k_G)H_m/k_c. \tag{7}$$

The equilibrium local mean curvature is then equal to (see equation (2)):

$$H^{\mathrm{eq}} = \big(C_1^{\mathrm{eq}} + C_2^{\mathrm{eq}}\big)/2 = C_1^{\mathrm{eq}} = C_2^{\mathrm{eq}} = k_cC_0/(2k_c + k_G) = H_m. \tag{8}$$

Microscopic theoretical models of biological membranes [5, 12] predict $k_c > 0$ and $k_G < 0$ therefore $K_1 > 0$ and $K_2 < 0$.

3. Determination of equilibrium shapes of closed thin anisotropic membranes with constant relative volume

In the following, the shape equation [7, 17] for a closed axisymmetric anisotropic membrane will be derived. The principal systems of the actual local membrane curvature tensor and the intrinsic membrane curvature tensor are assumed to coincide everywhere on the surface so that $\omega = 0$. Therefore equation (6) transforms in [18]

$$w = (2K_1 + K_2)(H - H_m)^2 - K_2(D - D_m)^2, \tag{9}$$

where $K_2 < 0$. The local stability condition for a small and completely free patch of the isotropic membrane demands $(2K_1 + K_2) > 0$, i.e., $K_1 > -K_2/2$, which is equivalent to the above derived Helfrich local stability condition $k_c > -k_G/2$. Based on the results of

microscopic theoretical models of biological membranes which show that Helfrich's constants k_c and k_G are of the same order of magnitude and that $k_G < 0$ [5, 12], and by taking into account the above-discussed isotropic limit of our model which gives $k_c = K_1$ and $k_G = K_2$ we take in the following for the sake of simplicity that $K_2 \sim -K_1$, therefore

$$w = K_1(H - H_m)^2 + K_1(D - D_m)^2. \tag{10}$$

To obtain the free energy of the whole membrane the integration of w over the membrane area A is performed so that

$$W = \frac{K_1}{4} \int ((2H - 2H_m)^2 + (2D - 2D_m)^2) \, dA. \tag{11}$$

For the sake of clarity, we introduce dimensionless quantities

$$h = R_s H, \qquad d = R_s D, \qquad h_m = R_s h_m, \qquad d_m = R_s D_m, \tag{12}$$

and

$$da = dA \big/ 4\pi R_s^2, \tag{13}$$

where the unit of length R_s is the radius of the sphere having its area equal to the total area of the membrane (A): $R_s = \sqrt{A/4\pi}$. Dividing the energy W by $4\pi K_1$ yields a dimensionless energy

$$\tilde{w} = \frac{1}{4} \int ((2h - 2h_m)^2 + (2d - 2d_m)^2) \, da. \tag{14}$$

To describe the closed axisymmetric membrane shape we introduce the coordinates $\rho(l)$ and $z(l)$ where ρ is the distance between the symmetry axis and a certain point on the contour, z is the position of this point along the symmetry axis and l is the arclength along the contour. The angle $\psi(l)$ made by surface normal and the z-axis is defined by the equation $\psi = dz/d\rho$ [7, 19]. Thus we can write h, d and da in a dimensionless form as

$$2h = \sin\psi/\rho + \psi_l, \tag{15}$$

$$2d = \sin\psi/\rho - \psi_l, \tag{16}$$

$$da = \frac{\rho}{2} \, dl, \tag{17}$$

where $d\psi/dl \equiv \psi_l$ and ρ, z and l are also dimensionless. Using the above equations (15)–(17) expression (14) gives

$$\tilde{w} = \frac{1}{8} \int \left(\frac{\sin\psi}{\varrho} + \psi_l - 2h_m \right)^2 \rho \, dl + \frac{1}{8} \int \left(\frac{\sin\psi}{\varrho} - \psi_l - 2d_m \right)^2 \rho \, dl. \tag{18}$$

In the following, the membrane shape with the minimal normalized elastic free energy $\tilde{w}$ at given relative area $a = A/4\pi R_s^2 = 1$, given relative volume $v = 3V/4\pi R_s^3 = v_0$ and given relative average mean curvature $\langle h \rangle = R_s \langle H \rangle$, where [20]:

$$\langle H \rangle = \frac{1}{A} \int H \, dA, \tag{19}$$

is obtained by minimizing the functional

$$G = \tilde{w} + \lambda_a a + \lambda_v v + \lambda_h \langle h \rangle. \tag{20}$$

The Lagrange multipliers λ_a, λ_v and λ_h can be determined from the constraints for the relative area, relative volume and the relative average mean curvature of the vesicle:

$$\frac{1}{2} \int \rho \, dl = 1, \tag{21}$$

$$\int \frac{3}{4} \rho^2 \sin \psi \, dl = v_0, \tag{22}$$

$$\frac{1}{4} \int \left(\frac{\sin \psi}{\varrho} + \psi_l \right) \rho \, dl = \langle h \rangle. \tag{23}$$

Using the definition

$$G = \int \mathcal{L} \, dl, \tag{24}$$

it follows from equations (18)–(24) that

$$\mathcal{L} = \frac{\rho}{8} \left(\frac{\sin \psi}{\varrho} + \psi_l - 2h_m \right)^2 + \frac{\rho}{8} \left(\frac{\sin \psi}{\varrho} - \psi_l - 2d_m \right)^2$$

$$+ \lambda_a \frac{\rho}{2} + \lambda_v \frac{3}{4} \rho^2 \sin \psi + \lambda_h \frac{\rho}{4} \left(\frac{\sin \psi}{\varrho} + \psi_l \right) + \lambda(\rho_l - \cos \psi). \tag{25}$$

The restriction for the geometrical relations between the angular coordinate ψ and the coordinate ρ ($\rho_l = \cos \psi$) was taken into account by introducing the additional Lagrange multiplier λ [21, 17, 19]. The Lagrange–Euler equations for the described variational problem are

$$\frac{\partial \mathcal{L}}{\partial \rho} - \frac{d}{dl} \left(\frac{\partial \mathcal{L}}{\partial \rho_l} \right) = 0, \qquad \frac{\partial \mathcal{L}}{\partial \psi} - \frac{d}{dl} \left(\frac{\partial \mathcal{L}}{\partial \psi_l} \right) = 0. \tag{26}$$

Equations (25) and (26) give the system of first-order differential equations:

$$\frac{d\lambda}{dl} = \frac{(\chi^2 - \sin^2 \psi)}{4\rho^2} + \frac{1}{2} \left(h_m^2 + d_m^2 \right) + \frac{\chi}{2\rho} (d_m - h_m) + \frac{\lambda_a}{2} + \frac{3}{2} \lambda_v \varrho \sin \psi + \lambda_h \frac{\chi}{4\rho}, \tag{27}$$

$$\frac{d\chi}{dl} = \frac{\sin \psi \cos \psi}{\rho} + 2\lambda \sin \psi - 2d_m \cos \psi + \frac{3}{2} \lambda_v \varrho^2 \cos \psi, \tag{28}$$

$$\rho_l = \cos \psi, \tag{29}$$

$$\psi_l = \chi / \rho. \tag{30}$$

The system of equations (27)–(30) is solved numerically, where the contour of the cell shape is determined using the relation

$$\frac{dz}{dl} = -\sin \psi. \tag{31}$$

The integration over the arclength l is performed from both poles so that the relative area of the calculated shape is equal to 1. Then, the validity of the constraints is tested and new initial values of the above quantities are set. The procedure is repeated until the constraints and the smoothness of the variables at the meeting point are fulfilled up to a prescribed accuracy.

In this above-described variational procedure the additional constraint for $\langle h \rangle$ was added due to practical reasons in order to better understand the nature of the calculated shape transitions. Therefore the final equilibrium value of $\langle h \rangle$ and the corresponding equilibrium shape with minimal energy $\tilde{w}$ was determined by additional minimization of the free energy of the shapes obtained by the solution of the above system of differential equations (equations (27)–(30)) over all possible values of $\langle h \rangle$ (see figure 2).
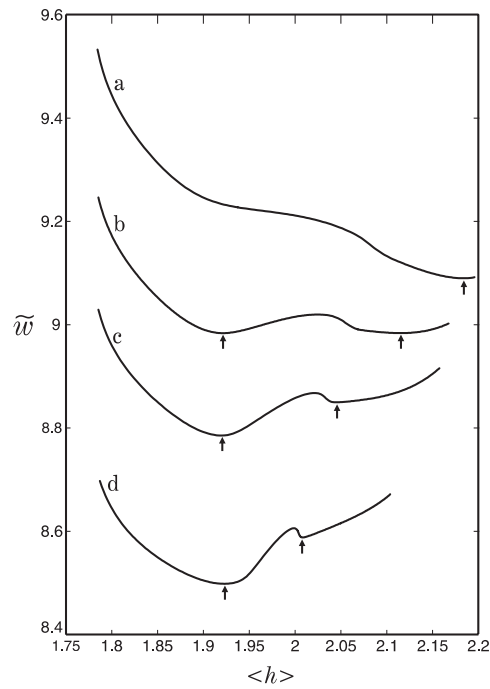
Figure 2. Membrane free energy of the shapes obtained in the variational procedure $\tilde{w}$ as a function of the average mean curvature $\langle h \rangle$ for different values of d_{m}: 0.1 (*a*), 0.2085 (*b*), 0.3 (*c*) and 0.4 (*d*). The values of other parameters are $v = 1/5^{1/2}$ and $h_{\mathrm{m}} = 4.5$. Arrows denote the local minima.
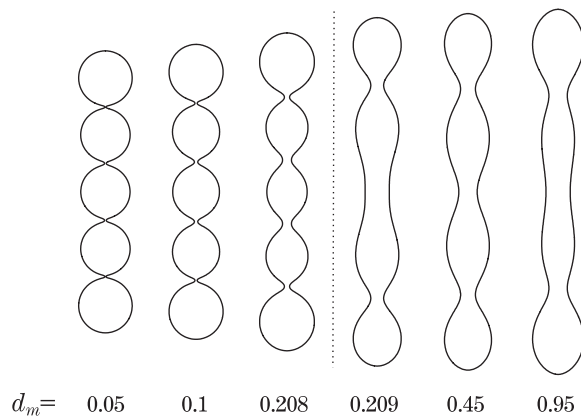
Figure 3. Calculated shapes determined by the minimization of the membrane free energy as a function of the intrinsic (spontaneous) curvature deviator of the membrane d_{m} for $v = 1/5^{1/2}$ and $h_{\mathrm{m}} = 4.5$.

4. Results and discussion

As an illustrative example, the described theory of the bending of closed anisotropic membranes (shells) is applied to study the nature of the shape transitions for closed membranes of undulated tubular shapes [22]. Figure 3 thus shows the calculated stable undulated

$h_m =$ 2.5   3.5   4.20   4.21   4.25
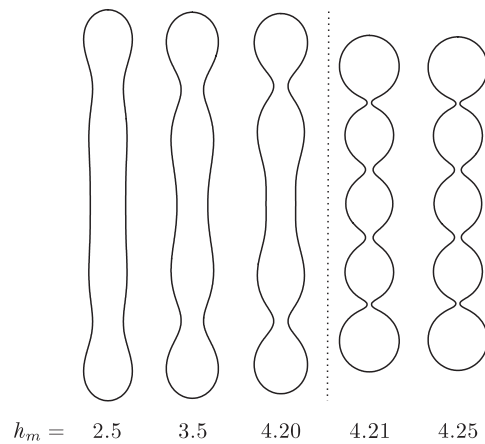
Figure 4. Calculated shapes determined by the minimization of the membrane free energy as a function of the intrinsic (spontaneous) mean curvature of the membrane h_m for $v = 1/5^{1/2}$ and $d_m = 0.1$.

tubular shapes as a function of the increasing intrinsic (spontaneous) curvature deviator of the membrane (d_m) for a given relative volume v and a given intrinsic (spontaneous) mean curvature h_m. It can be seen in figure 3 that the calculated shapes continuously elongate with increasing d_m until the critical value of d_m is reached where the shape is changed discontinuously to a less undulated shape. For small $d_m \rightarrow 0$ the shape approaches the limiting shape [23] comprising equal spheres connected by infinitesimally thin necks (figure 3).

The shapes within the calculated cell shape sequence strongly depend on the values of the cell relative volume v. At smaller relative volumes v the cells are more elongated and therefore the limiting shapes comprise a larger number of beads (spheres) [23]. In this case one can also observe the discontinuous shape transitions between 6 and 5, 7 and 6 beads etc and after the discontinuous transition the series of continuous transitions driven by increasing d_m.

The predicted discontinuous shape transition (figure 3) can be understood by studying the dependence of the membrane energy determined in the variational procedure $\tilde{w}$ (equation (14)) on the average mean curvature $\langle h \rangle$ for different values of d_m at a chosen value of h_m. It can be seen in figure 2 that at low values of d_m the function $\tilde{w}(\langle h \rangle)$ has only one minimum at larger $\langle h \rangle$ (curve (a)) corresponding to a strongly undulated shape which resembles a chain of beads (bead-like shapes). With increasing d_m, a second (left) minimum appears at smaller $\langle h \rangle$ which corresponds to a less undulated, more tubular shape (curve (b)). For small enough d_m this second minimum does not correspond to the absolute minimum. However, with increasing d_m at a critical value of d_m the second (left) minimum of $\tilde{w}(\langle h \rangle)$ also becomes the absolute minimum. The corresponding shape transition from a bead-like shape to a less undulated shape is therefore discontinuous (figure 3).

For comparison, figure 4 shows the dependence of the calculated undulated tubular shape on the intrinsic (spontaneous) mean curvature h_m for given values of d_m and v. Again, a dramatic change of the stable shape can be observed at a certain critical value of h_m where the smooth prolate shape discontinuously transforms into a strongly undulated shape which resembles a chain of beads connected by thin necks. The calculated discontinuous shape transition can, therefore, be referred to as a beading transition. For the sake of simplicity the

non-local bending of the membrane bilayer [4, 24] and the shear elasticity of the membrane skeleton [25, 26] are not considered in this work.

In biological systems, the beading transition of nerve fibres was observed recently [13]. The beading of nerve fibres was induced by mild stretching [13] and seems to be independent of the cytoskeleton and myelin sheath, leading to the conclusion that the membrane bilayer or the membrane skeleton (connected via transmembrane proteins to the extracellular matrix) plays a key role in stretching induced beading of the nerve fibres [13]. In accordance, it was shown theoretically that the change of the lateral tension in the lipid bilayer of the axon membrane (or the change of the transmembrane pressure difference) may induce beading of the nerve fibres [27]. Whether this beading has functional consequences is unknown so far. However, since it has also been observed during Wallerian degeneration [13] one cannot exclude a possibility that beading also accompanies the damage afflicted to nerve fibres.

Beaded nerve fibres have also been observed in the absence of stretching of nerve fibres [13, 14]. This implies that besides the change of the membrane tension or transmembrane pressure there are also other possible (yet unknown) mechanisms which may induce beading of the nerve fibre [27]. In accordance, it has been shown recently that the beading of nearly cylindrical nerve fibres can also be induced by internalization of the membrane receptors of substance P [28, 29]. During internalization of these receptors (involving their encapsulation and endovesiculation) the area of the inner layer is reduced to a larger extent than the area of the outer layer of the membrane bilayer of the axon [28, 29]. As a consequence, the area difference between the outer and the inner layer of the parent membrane bilayer is increased. In the mathematical model, this increase of the area difference can be taken into account as the increase of the membrane effective spontaneous curvature [26, 29], or in our model, as an increase of the intrinsic mean curvature h_m which may induce the beading transition for $d_m \neq 0$ (figure 4). Figure 4 shows that already a small increase in h_m may lead to beading shape transition as observed also in experiments [28, 29]. The assumed anisotropy of the membrane bilayer and its skeleton (i.e., the non-zero value of the intrinsic (spontaneous) curvature deviator d_m) may be the consequence of orientational ordering of the constituents of the membrane bilayer (proteins and lipids) [10, 30, 12]. The possible origin of the anisotropy of the membrane of the nerve fibres (composed of the membrane bilayer and the membrane skeleton) can also be weak longitudinal orientation of the membrane skeleton elements. We described the mechanical properties of such anisotropic membrane in the first approximation by the intrinsic (spontaneous) curvature deviator of the membrane d_m and the intrinsic (spontaneous) mean curvature h_m, as suggested above (see equation (10)).

It is possible that in the process of beading of the nerve fibres which is not induced by stretching [13, 14] also the myelin sheath, which undergoes the beading transition together with the axon membrane, may play an important role. The myelin sheath is composed of $\sim$70% of lipids and $\sim$30% of proteins. The myelin membrane [31] is wound around the axon like an insulating tape around a wire. Therefore in cross-section the myelin sheath appears as a multilayered membrane structure [13, 27] which can be considered as anisotropic due to its specific structure (see also [3]).

To conclude, thin membranes and strips are in general not flat when they are in the state of minimal free energy. The preference of thin isotropic membranes and strips for bent states is usually mathematically characterized by a material constant called spontaneous curvature C_0 [4, 22]. In the case of bilayer membranes, the effective spontaneous curvature was introduced in order to take into account also the contribution of asymmetry (in the area, composition and environment) between both layers of the membrane bilayer [4, 26, 32]. The corresponding elastic free energy per unit area may then be written in the form of equation (1) [4]. In contrast to the case of isotropic membranes and strips, the preference of anisotropic membranes and

strips for the bent state is described with two intrinsic parameters, intrinsic (spontaneous) mean curvature H_m and intrinsic (spontaneous) curvature deviator D_m (equation (6)).

In the past, the membrane beading (pearling instability) produced by sudden tension in the membrane tubes induced by laser tweezers has been studied within the theoretical model which takes into account the membrane surface tension and Helfrich isotropic membrane bending energy [33]. Similar theoretical models were used also to theoretically describe membrane beading due to the incorporation of molecules in the membrane bilayer [32] and membrane beading in aging blood cells [22] where a second-order beading transition of cylindrical membrane structures was predicted for non-zero membrane spontaneous curvature C_0. In the present work, we predicted the first-order beading transition (figures 3 and 4) within the generalized spontaneous curvature model (without the in-plane membrane stretching energy contribution) where the preference of anisotropic membrane for the bent state is described by two intrinsic parameters (H_m and D_m) instead by only one spontaneous curvature C_0 that was used in previous works regarding laterally isotropic membranes.

In the spontaneous curvature model [7] the equilibrium shapes of closed membranes depend on the normalized cell volume v and on (effective) spontaneous curvature C_0 which is connected to intrinsic (spontaneous) mean curvature h_m) introduced in our model. In this work, we propose an extension of the phase diagram of the spontaneous curvature model into the dimension of the intrinsic (spontaneous) curvature deviator d_m. The proposed extension of the phase diagram of the closed membrane shapes in the third dimension (in the direction of the coordinate d_m as shown in figure 3) represents a generalization of the spontaneous curvature model for isotropic membranes.

Acknowledgments

References

[1] Helfrich W and Prost J 1988 *Phys. Rev.* A **15** 3065
[2] Oda R, Huc I, Schmutz M, Candau S J and MacKintosh F C 1999 *Nature* **399** 566
[3] Kralj-Iglič V, Remškar M, Vidmar G, Fošnarič M and Iglič A 2002 *Phys. Lett.* A **296** 151
[4] Helfrich W 1974 *Z. Naturf.* **29c** 510
[5] Ben-Shaul A 1995 *Structure and Dynamics of Membranes* ed R Lipowsky and E Sackmann (Amsterdam: Elsevier)
[6] Srolovitz D J, Safran S A, Homyonfer M and Tenne R 1995 *Phys. Rev. Lett.* **74** 1779
[7] Deuling H J and Helfrich W 1996 *J. Physique* **37** 1335
[8] Chung D O, Benedek G B, Konikoff F M and Donovan J M 1993 *Proc. Natl Acad. Sci. USA* **90** 11341
[9] Selinger J V, MacKintosh F C and Schnur J M 1996 *Phys. Rev.* E **53** 3804
[10] Fournier J B 1996 *Phys. Rev. Lett.* **76** 4436
[11] Kralj-Iglič V, Heinrich V, Svetina S and Žekš B 1999 *Eur. Phys. J.* B **10** 5
[12] Kralj-Iglič V, Iglič A, Gomišček G, Sevšek F, Arrigler V and Hägerstrand H 2000 *J. Phys. A: Math. Gen.* **70** 1533
[13] Ochs S, Pourmand R, Jersild R A and Friedman R A 1997 *Prog. Neurobiol.* **52** 391
[14] Allen B J, Rogers S D, Ghilardi J R, Menning P M, Kuskovsky M A, Basbaum I, Simone D A and Manthy P W 1997 *J. Neurosci.* **17** 5921
[15] Iglič A, Tzaphlidou M, Remškar M, Babnik B, Daniel M and Kralj-Iglič V 2005 *Fullerenes, Nanotubes and Carbon Nanostructures* **13** 183
[16] Landau L D and Lifshitz E M 1997 *Theory of Elasticity* 3rd edn (Oxford: Butterworth-Heinemann)
[17] Jülicher F and Seifert U 1994 *Phys. Rev.* E **49** 4728
[18] Fischer T M 1992 *J. Physique* II **2** 337

[19] Zhong-Can Ou-Yang, Ji-Xing Liu and Yu-Zhang Xie 1999 *Geometrical Methods in Elastic Theory of Membranes in Liquid Crystal Phases* (Princeton, NJ: World Scientific)

[20] Evans E A and Skalak R 1980 *Mechanics and Thermodynamics of Biomembranes* (Boca Raton, FL: CRC Press)

[21] Heinrich V 1991 Theoretische Bestimmung von kugelnahen Vesikelfomen mit Hilfe von Kugelfunktionen *PhD Thesis* Humboldt University, Berlin

[22] Deuling H J and Helfrich W 1977 *Blood Cells* **3** 713

[23] Iglič A, Kralj-Iglič V and Majhenc J 1999 *J. Biomech.* **32** 1343

[24] Miao L, Seifert U, Wortis M and Döbereiner H G 1994 *Phys. Rev.* E **49** 5389

[25] Iglič A 1997 *J. Biomech.* **30** 35

[26] Mukhopadhyay R, Lim G and Wortis M 2002 *Biophys. J.* **82** 1756

[27] Markin V S, Tanelian D L, Jersild R A and Ochs S 1999 *Biophys. J.* **76** 2852

[28] Mantyh P W, Allen C J, Ghilardi J R, Rogers S D, Mantyh C R, Liu H, Basbaum A I, Vigna S R and Maggio J E 1995 *Proc. Natl Acad. Sci. USA* **92** 2622

[29] Tanelian D L and Markin V S 1997 *Biophys. J.* **72** 1092

[30] Kralj-Iglič V, Iglič A, Hägerstrand H and Peterlin P 2000 *Phys. Rev.* E **61** 4230

[31] Ohler B, Graf K, Bragg R, Lemons T, Coe R, Genain C, Israelachvili J and Husted C 2003 *Biochim. Biophys. Acta* **1688** 10

[32] Chaieb S and Rica S 1998 *Phys. Rev.* E **58** 7733

[33] Bar-Ziv R and Moses E 1994 *Phys. Rev. Lett.* **73** 1392